Measurements of low-level prepulse on Nike KrF laser.*

Max Karasik,† A. N. Mostovych, R. H. Lehmberg, Y. Chan, J. L. Weaver, and S. P. Obenschain
Plasma Physics Division, Naval Research Laboratory
Washington DC 20375

The krypton fluoride (KrF) laser is a leading candidate driver for inertial fusion energy. Some of the current fusion target designs call for targets with thin metallic coatings. These targets could be particularly susceptible to preheat by a low-level laser prepulse. Knowledge of the prepulse can be important in understanding and modeling the behavior of such targets. This paper presents measurements of low-level prepulse on target with the Nike KrF laser. Sources of prepulse are discussed and measurements are performed under several specific laser conditions in order to evaluate the relative contribution of these sources to the overall prepulse. Prepulse is found to be $\sim 2\times10^{-7}$ from peak intensity for approximately 120 ns prior to the main laser pulse. Prepulse energy density on target is ~ 2 J/cm^2. The first laser amplifier in the time- and angle-multiplexed section of the laser is found to be the dominant source of prepulse.

PACS numbers: 42.55.Lt, 42.60.-v,42.60.Jf, 52.57.-z, 89.30.Jj

I. INTRODUCTION

The krypton fluoride (KrF) laser is a leading candidate driver for inertial fusion energy[1]. Its capability to achieve ultra uniform high energy illumination of targets with short wavelength laser light also makes a KrF laser valuable for experiments. The Nike KrF laser facility[2] is used to conduct planar target experiments. Up to 44 overlapped beams are used to illuminate the main target with high uniformity. The laser is designed to produce high contrast ($\sim 10^7$ in intensity) pulses. Recent experiments have found[3] that the use of thin metallic layers on the laser side of the target can reduce the transfer of laser non-uniformity to the target, known as laser imprint. The thin (100–1000 Å) metallic layers initially absorb most of the laser light, and because of their low areal mass density can be significantly heated even by a relatively low-level prepulse that reaches the target before the main pulse. In the case of such targets, knowledge of the prepulse intensity vs. time can be important in understanding and accurately modeling the subsequent laser-target interaction.

Prepulse has been a particular concern for short pulse (~ 100 fs) high intensity lasers, where even a 10^7 contrast could mean 10^{12} W/cm^2 intensity on target prior to the main pulse[4]. Techniques have been developed to perform prepulse measurements on such lasers[5]. However, such methods are not directly applicable to high energy, long pulse, many-beam lasers used in inertial confinement fusion research, such as Nike.

Previous prepulse measurements on Nike[2] were conducted either at low power (front end of the laser only) or indirectly at full power by side-on imaging of the target just prior to the main pulse or by monitoring the front surface temperature[6]. Prepulse is measured at full power for several individual beams by light pickoff, however measurement of all 44 beams individually is impractical. Direct measurements of the prepulse at full power at the target are complicated by the fact that any laser-facing elements of the diagnostic would be destroyed after the arrival of the main pulse, producing potentially damaging debris in the target chamber. In this paper, a prepulse diagnostic is described that circumvents this problem. Direct full power measurements of the prepulse are presented for several specific laser operating conditions. The paper is organized as follows. Sources of prepulse in Nike's optical and amplifier train are discussed in Section I A. Details of the measurement setup are given in Section II. Measurement results and prepulse dependence on various laser conditions are presented in Section III, followed by a discussion of the results in Section IV. Finally, conclusions are drawn in Section V.

A. Sources of prepulse

On Nike laser, prepulse occurring within 10 ns of the main pulse is dominated by the pulse shaping and amplification in the front end of the laser prior to beam multiplexing, is present on all the beams, and is measured on each shot as part of the pulse shape. The front end consists of an oscillator and amplifiers that utilize discharge pumping with ~ 20 ns gain durations. Leakage through the Pockels cell shutters results in prepulse arriving on target starting at ~ 20 ns prior to the laser pulse. Earlier than ~ 20 ns, the amplifiers are completely off and there is no appreciable prepulse from the front end.

Prepulse arriving to the target at earlier times has its origins in the angularly multiplexed electron beam pumped amplifiers. This early time prepulse is different for each individual beam and has two sources: amplified spontaneous emission (ASE) from the electron beam pumped amplifiers and beam-to-beam scatter (BBS) in optics in which individual beam paths overlap. It is this early time prepulse, hereafter referred to simply as pre-

*To appear in J. Appl. Phys. Aug 15,2005
†Electronic address: karasik@nrl.navy.mil

pulse, that is the subject of this paper. Details of Nike optical train and amplifier staging are given elsewhere[2]. The two sources of prepulse are discussed in detail in this section.

Nike has two electron beam pumped amplifiers with 20 cm and 60 cm square apertures, hereafter referred to as the 20cm and 60cm amplifiers (refer to Figure 1). The amplifiers are on for approximately 160 ns and 300 ns, respectively. During these times, 28 beams in the case of the 20cm and 56 beams in the case of the 60cm are sent through the amplifiers sequentially and at slightly different angles (time and angle multiplexing). The 28 beams multiplexed through the 20cm amplifier go through a beamsplitter, creating 56 beams which are then sent through the 60cm amplifier in two sets: the first half (beams 1-28) and the second half (beams 29-56). The second half of the beams is delayed with respect to the first half to go through the amplifier in sequence. In order for all the beams to arrive at the target simultaneously, each subsequent beam has a shorter path length to the target after the amplifiers than the previous one. Six of the beams going through the 20cm amplifier and twelve of the beams going through the 60cm amplifier are diagnostic beams used for backlighting and are of 5.3 ns duration; the rest of the beams are for driving the target and are 4 ns long. The amplifiers are on longer than the total duration of the beams (120 ns and 240 ns, respectively) to allow for finite turn-on time and jitter.

Of the two amplifiers, the 20cm is expected to have a stronger contribution to the prepulse intensity on target from both the ASE and BBS components. As will be shown below, this is because the ASE originating in the 20cm is amplified by the 60cm and because the BBS intensity on target scales inversely with the square of the amplifier aperture.

The location of the amplifiers far from the image planes of the laser relay optics results in a reduced prepulse intensity on target as the ASE and BBS originating at the amplifiers is not focused in the target plane.

1. ASE

While the two amplifiers are on, ASE from them illuminates the optics that collect the individual laser beams (Figure 2a). ASE produced at a particular time in the amplifier gain window and collected by the optics for the beams that have not yet gone through the amplifier reaches the target prior to the arrival of the laser beams, thus contributing to the prepulse. The contribution to the prepulse is particularly strong at the beginning of the amplifier gain window when the amplifier is not yet being loaded up by the laser beams and all the light collected by the individual beam optics arrives at the target early, albeit at various times. The ASE from the end of the gain window arrives at the target after the laser beams and thus does not contribute to the prepulse.

The time that the ASE from each of the two amplifiers

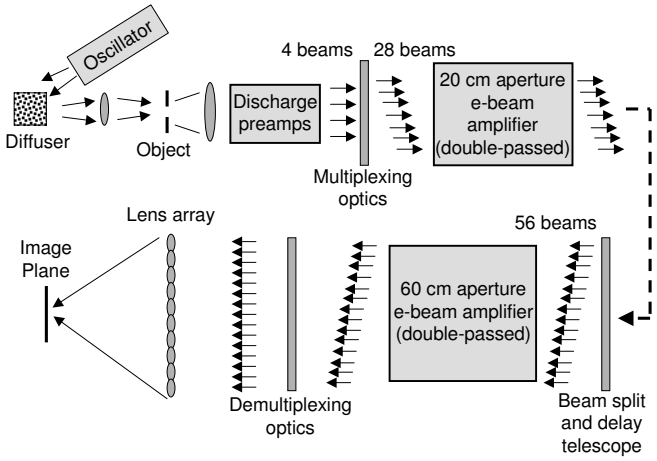

FIG. 1: Optics and amplifier staging.

begins to arrive on target prior to the main pulse is determined as follows. The ASE begins when the amplifier first turns on. Because of time multiplexing, its shortest path to target is along the path of the last laser beam to go through the amplifier. Thus the earliest ASE makes it to target earlier than the laser pulse by the time difference between the amplifier turn-on and the time the last beam exits the amplifier. In the case of the 20cm amplifier, this time is approximately 155 ns; for the 60cm amplifier, it is approximately 285 ns.

Calculations of ASE radiance at the amplifiers and intensity on target for a time multiplexed electron beam pumped KrF system are given in Ref. 7. There, peak ASE intensity on target due to a single amplifier is given by:

$$I = \kappa G G_{tot} T N \frac{1}{f^2}, \tag{1}$$

where G is the amplifier gain, $G_{tot} = G_1 G_2 \ldots$ is the product of any subsequent stage gains, T is the optical transmission from the amplifier to the target, N is the number of beams multiplexed through the amplifier that end up on target, f is the ratio of the focal length to the beam width at the final focusing lens (effective f-number), and κ is a coefficient weakly dependent on the amplifier gain[7]:

$$\kappa \approx \frac{h\nu}{4\pi\sigma\tau_R}\left(\frac{1}{1-\chi}\right)\left[\frac{4}{\pi}\ln\left(\frac{\ln G}{\ln G/2}\right)\right]^{1/2}. \tag{2}$$

Here, $h\nu$ is the photon energy, $\sigma = 2.6 \times 10^{-16}$ cm^2 is the stimulated emission cross-section, and $\tau_R = 6.5$ ns is the spontaneous radiative lifetime. $\chi = \alpha/n\sigma \approx 1/7$, where α is the loss coefficient and n is the number density of excited KrF molecules. Physically, κ can be seen as a spontaneous emission radiance to be amplified: $h\nu/4\pi\sigma\tau_R = (nh\nu/4\pi\tau_R) \times (1/n\sigma)$ =(spontaneous radiated power density per steradian)×(mean free path for

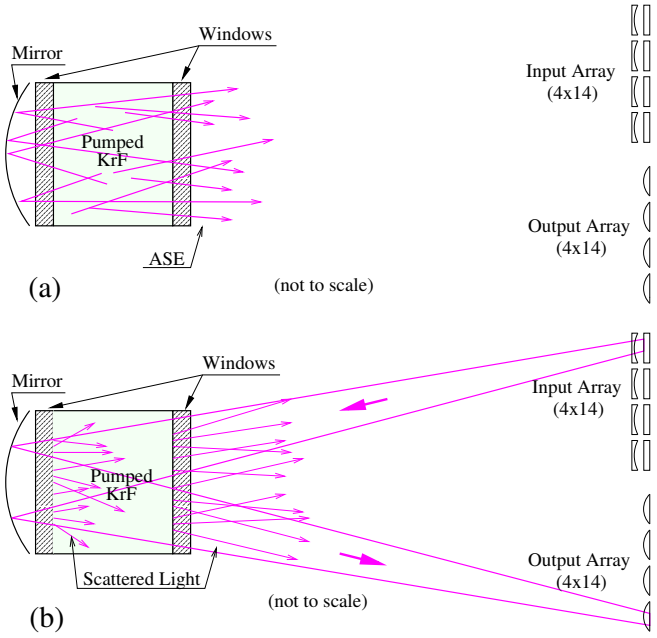

FIG. 2: The two sources of prepulse. (a) Amplified Spontaneous Emission (ASE). For clarity the laser beams are not shown. Some of the ASE is collected by the output array optics and makes it to the target. ASE collected by the output array optics with the shortest path to target (late beams) arrives to the target earliest. (b) Beam-to-Beam Scatter (BBS). Scattering arises primarily on the inner surfaces of the amplifier windows after they have been etched by prolonged exposure to fluorine compounds. For clarity, only one of the 28 or 56 beams is shown. Also, scattering only in the direction of the arrays is shown, however scattering reflected in the mirror can also contribute. Scattered light from an input beam that is collected by the output array optics of subsequent beams will arrive to the target early.

a stimulated emission to occur). For a typical amplifier gain $G \sim 100$, $\kappa \approx 2 \times 10^4$ W/(cm$^2 \cdot$ str).

The time evolution of the ASE intensity on target due to each amplifier, assuming constant ASE radiance $\kappa G G_{tot}$, is a staircase ramp of the total duration of the beams on target τ (up to 88 ns and 176 ns for the 20cm and 60cm amplifiers, respectively) followed by constant intensity for τ_0, the time from the amplifier turn-on to the time the first target beam enters the amplifier. τ_0 includes the duration of the diagnostic backlighter beams which do not end up on target. The ASE energy density on target due to each amplifier is the time integral of intensity and is thus given as:

$$E = (\tau/2 + \tau_0)I. \quad (3)$$

Values of the relevant parameters for the 20cm and 60cm amplifiers and the corresponding peak ASE intensities and energy densities are given in Table I.

As can be seen from the calculated values of intensity in the table, the peak ASE intensity on target due to the 20cm amplifier is two orders of magnitude higher than

TABLE I: Values of the relevant parameters for the 20cm and 60cm amplifiers and the corresponding calculated peak ASE intensities and energy densities on target. The calculation assumes saturated gains for the amplifiers.

Parameter	20cm	60cm
Gain G	680	68
Transmission to target T	0.25	0.73
Number of target beams N (max)	2x22	44
f-number f	40	
ramp duration τ (ns)	88	176
constant ASE duration τ_0 (ns)	67	109
Peak intensity I (W/cm^2)	6.4×10^6	2.7×10^4
Energy density E (J/cm^2)	0.74	5.5×10^{-3}

that of the 60cm amplifier. This is due primarily to the ASE from the 20cm being amplified by the 60cm, and also due to the higher gain of the 20cm amplifier.

The above calculations assume saturated gains for the two amplifiers. This assumption is violated during the ramp-up of the amplifiers, when the amplifiers are not yet being loaded with incoming laser beams and the gains are much higher. Because of this, these calculations are approximately an order of magnitude lower than the measured values, as will be seen in Section III.

In order to obtain a more realistic estimate of the prepulse due to the ASE from the 20cm and 60cm amplifiers, the time-dependent gain of the two amplifiers was simulated using the NRL KrF kinetics code Orestes[8]. The simulation includes measured temporal profiles of the amplifiers as well as actual timing of the beams multiplexed through the amplifiers. The simulation yields a time-dependent product of the gains of the 20cm and 60cm amplifiers needed for the 20cm ASE calculation as well as the time-dependent gain of just the 60cm amplifier for calculating the ASE originating in the 60cm amplifier. To calculate the prepulse intensity on target due to ASE, the prepulse due to each beam is obtained by substituting these gains with appropriate time shift into Eq. 1 (with N set to 1), and summing over all the beams. An example of the time-dependent gain product is shown in Fig. 3. The prepulse intensity obtained in this way is plotted together with measured prepulse in Section III below.

2. BBS

Wherever angularly multiplexed beams overlap on an element in the optical train, scatter from imperfections in the optic can result in light from one beam being scattered into the paths of other beams. The primary source of BBS is scattering due to surface roughness of the coated amplifier windows and mirror. The inner surfaces of the windows are exposed to the harsh environment of fluorine compounds in the amplifiers. Over time they become etched and increasingly scatter the amplified light

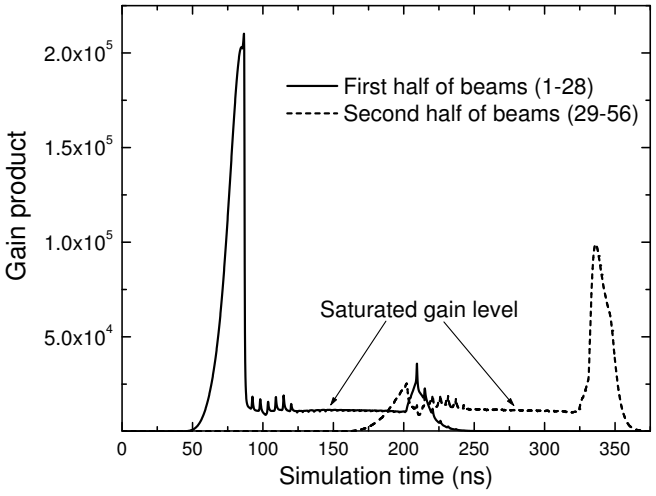

FIG. 3: Simulation of the product of amplifier gains and transmission for the first (beams 1-28) and second (beams 29-56) half of the beams. The prominent gain spikes at the beginning and at the end occur when the laser beams are not loading down the amplifiers. The plateaus in between are the product of saturated gains when the amplifiers are loaded with laser beams.

(minimizing presence of water in the laser chamber has been found to prolong the life of amplifier windows on Nike). Light from a particular beam, designed to be collected by a particular element of the output array, can thus be scattered into the path of another beam, as can be seen in Figure 2b. If this path is that of a beam that goes through the amplifier later than the current one, it will have a shorter distance to the target, and the scattered light will arrive to the target earlier than the main pulse, contributing to the prepulse.

BBS is expected to be largely due to small angle scattering. BBS from a particular beam is thus expected to mostly scatter into the paths of beams whose collection optics are nearby. The output arrays of the amplifiers are arranged so that beams that are nearby in angle are also close in time, minimizing the length of the prepulse on target due to BBS. Nevertheless, the earliest prepulse on target due to BBS will arrive on target earlier than the laser pulse by the time difference between the first beam and the last beam. For the 20cm and 60cm amplifiers, this time is approximately 120 ns and 240 ns, respectively.

BBS has been discussed in literature[9, 10], but only estimates of prepulse on target due to BBS are given. Furthermore, as mentioned in Ref. 9, there are no measurements of scattering characteristics of amplifier windows as they age in operation.

Scaling of BBS intensity on target with amplifier parameters can be made as follows using considerations similar to those used to derive Eq. 1. Intensity on target due to BBS scales as:

$$I_{BBS} \sim 4G_{tot}TW^2\mathcal{R}_{BBS}\Omega_T/A_T, \tag{4}$$

where G_{tot} is the gain of any subsequent amplifiers, T is as defined before, W is the aperture of the amplifier, A_T is the area of the target, and $\mathcal{R}_{BBS}$ is the BBS radiance at the output window of the amplifier. Ω_T is the solid angle subtended by the target as seen at the amplifier exit plane, given by[7]:

$$\Omega_T = \left(\frac{1}{fW}\right)^2 A_T, \tag{5}$$

where f is the effective f-number as defined before. The factor of 4 is due to the amplifier having two windows that are double passed. BBS radiance with its time dependence on target can be written in the form:

$$\mathcal{R}_{BBS} = \frac{P}{W^2}\sum_{i,j=1}^{N} s(\theta_{ij})\left[\Phi(t-(i-j)\tau_b) - \Phi(t-(i-j+1)\tau_b)\right], \tag{6}$$

where $s(\theta_{ij})$ is fractional power per unit solid angle scattered from beam i into beam j with θ_{ij} being the angle between the two beams, P is the laser light power out of the amplifier, τ_b is the duration of each beam, N is the number of beams as before, and the unit step function $\Phi(t) = 0$ for $t < 0$ and 1 for $t > 0$ with $t = 0$ corresponding to half-rise of the main pulse on target.

For the purposes of determining the relative importance of the two amplifiers in BBS intensity on target and without knowing the actual scattering function of the amplifier windows, Eq. 6 can be written as:

$$\mathcal{R}_{BBS} = S_N(t)P/W^2 \tag{7}$$

with $S_N(t)$ containing all the details of the scattering of the N beams. With the laser intensity on target $I_{laser} = NTPG_{tot}/A_T$, Eq. 4 becomes:

$$I_{BBS} \sim 4I_{laser}\Omega_T S_N(t)/N = 4I_{laser}\left(\frac{1}{fW}\right)^2 A_T S_N(t)/N. \tag{8}$$

BBS thus scales inversely with the square of the amplifier aperture. The 20cm amplifier is thus expected to have an order of magnitude higher BBS intensity on target than the 60cm amplifier.

II. MEASUREMENT SETUP

The setup used for measurement of prepulse is shown in Figure 4. Up to 44 Nike laser beams are focused and overlapped to a 750 μm spot in the target plane. A thin ($\sim 100\ \mu$m) 1″ dia. uncoated fused silica microscope coverslip is positioned approximately 1″ in front of the target plane. The reflection from it goes through a focus and is imaged using two $f = 1.8$ plano-convex lenses onto a photodiode. The fused silica coverslip acts as a fuse in the measurement apparatus. It has a high damage threshold ($\gtrsim 10$ J/cm^2) that allows measurement of prepulse to take place until just before the ramp-up of the main

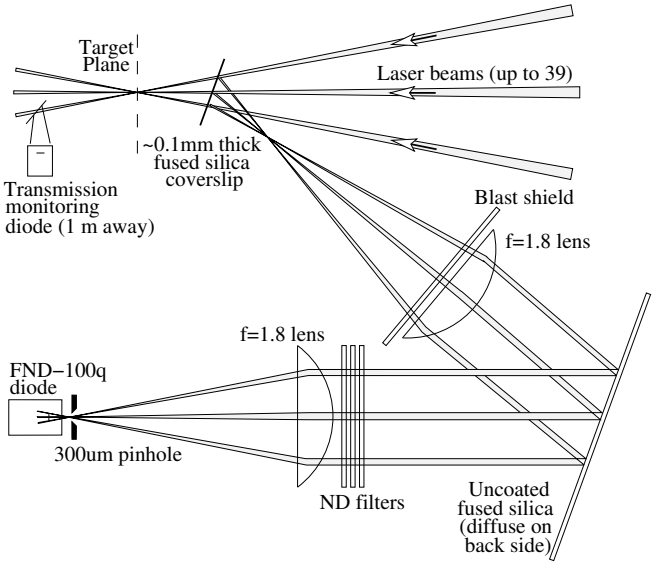

FIG. 4: Measurement Setup.

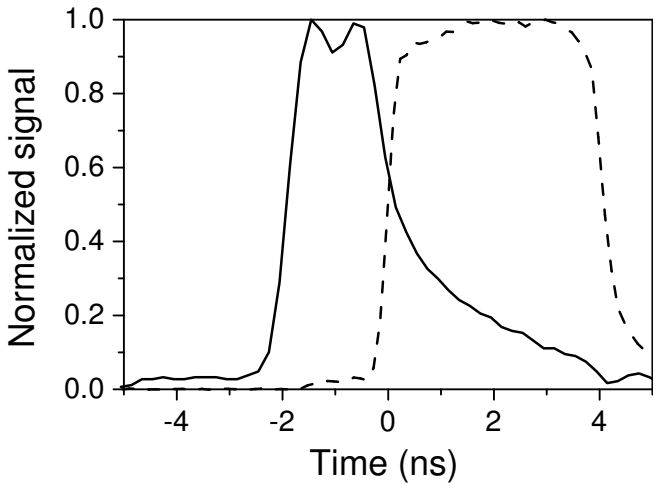

FIG. 5: Transmission through the fused silica coverslip (solid line). The dashed line is the laser pulseshape. The pulseshape had a 2% "foot" starting at approximately −2 ns. The coverslip remains transparent until it breaks down as the main laser pulse begins to ramp up at $t = -0.5$ ns.

pulse. Once the main pulse begins to ramp up, however, the coverslip breaks down and is no longer a specular reflector, limiting the flux to the rest of the optics. Since the thickness of the coverslip is comparable to that of targets normally used in experiments on Nike, the risk of shrapnel damage to the target chamber optics is not excessive.

The prepulse light is attenuated in order to keep the photodiode out of saturation. This is accomplished by placing an uncoated fused silica reflector followed by neutral density (ND) filters between the two lenses. The reflector is diffuse on the rear side, eliminating the second Fresnel reflection and diffusing the transmitted light to eliminate the need for a beam dump. The total transmission from the target plane to the relayed image plane is approximately $8\%\times4\%\times1\%=3\times10^{-5}$, where the 8% is due to Fresnel reflection from the coverslip, the 4% is one Fresnel reflection from the fused silica reflector, and the 1% is the ND filter transmission. The ND filters can be removed for measuring the lowest prepulse levels.

The sensitive area of the photodiode is 2.5 mm in diameter, and is larger than the 750 μm laser spot size. A pinhole 300 μm in diameter is placed at the imaged target plane in front of the photodiode in order to precisely define the measurement area. The photodiode diameter was chosen to be larger than the laser spot size in order to collect all the imaged laser light during calibration (see below). The pinhole diameter was chosen to be smaller than the 400 μm flat-top of the 750 μm FWHM laser spot size to have a continuous intensity measurement from the early time prepulse to the time when the main pulse begins to ramp up. On the other hand, the pinhole had to be sufficiently large to allow enough prepulse light to have a good signal on the photodiode for the lowest prepulse levels.

Prepulse is expected to be uniform over the 300 μm diameter of the pinhole because of the following. Both ASE and BBS originate at the laser amplifiers, which are located near the Fourier planes of the imaging optics used to transport the Nike beams. Prepulse is therefore not focused in the target plane and so is not expected to vary spatially over the laser spot size. To verify prepulse uniformity, shots were taken with the pinhole-photodiode assembly translated ±1 mm left-right and up-down in the imaged target plane. No secular trend was found; only the usual shot-to-shot variation.

The time at which the coverslip breaks down is monitored using the coverslip transmission monitoring photodiode, also shown in Figure 4. An uncoated fused silica plate approximately 1 m behind the coverslip is used to pick-off light from one of the laser beams transmitted through the coverslip and reflect it into the photodiode. During a shot, light from the beam reaches the photodiode until the coverslip breaks down and stops transmitting. A typical signal from this photodiode is shown in Figure 5. Overlaid on the figure is the laser pulseshape for that shot. As can be seen in the figure, the photodiode signal begins to fall only after $t = -0.5$ ns, while the laser pulse is ramping up. It is thus reasonable to assume that the coverslip retains Fresnel reflection through the time of interest for the prepulse measurement, i. e. for times earlier than $t = -10$ ns.

A. Absolute calibration

The measurement apparatus is calibrated *in situ* as follows. A sensitive calorimeter (∼10 V/J) is placed just behind the target plane to capture all the laser light

transmitted through the coverslip. The pinhole is removed from in front of the photodiode in order to collect all the imaged light. The front end of the laser is fired, with approximately 1 mJ reaching the coverslip. The pulse length is set to approximately 12 ns, which is longer than the photodiode response time (∼3 ns). The energy in the pulse is measured using the calorimeter and corrected by the transmission of the coverslip (measured to be 92% at 248 nm using a spectrophotometer). The waveform from the photodiode is numerically integrated. The ratio of the pulse energy to the integral of the photodiode waveform gives the calibration factor (Watts on target)/(photodiode Volts) for the apparatus. Finally, dividing this calibration factor by the area of the 300 μm pinhole used during the prepulse measurement gives the calibration in terms of intensity on target per volt of the photodiode signal.

In order to obtain the prepulse level relative to peak laser pulse intensity, the prepulse intensity is normalized by the main laser pulse intensity. The latter is obtained in the usual manner by measuring the laser energy using calorimeters, pulse duration using the pulse-shape diagnostics, and spot size by beam profile measurement on target.

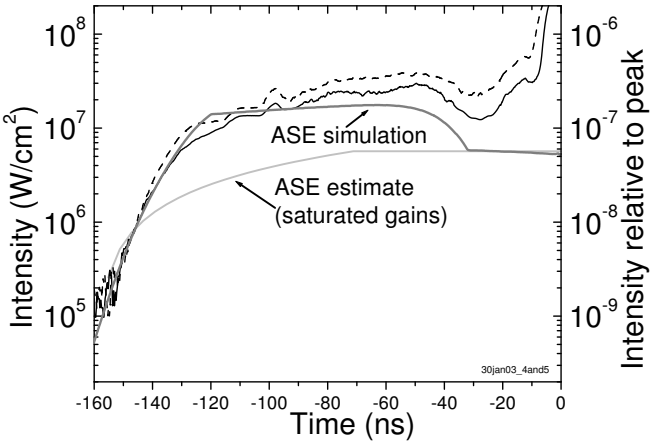

FIG. 6: Measured prepulse for two shots: 39 beams, new windows on the 20cm and 60cm amplifiers; standard amplifier timing. The ∼ 50% variation between the two shots is typical of the prepulse shot-to-shot variation. Also shown is a theoretical estimate of the prepulse from ASE only, assuming saturated gain in the amplifiers, as well as a simulation of ASE that includes the higher gain while the amplifiers are still unloaded. In this and subsequent figures unless noted $t = 0$ refers to the time at which the laser pulse reaches 1/2 of its peak intensity.

III. PREPULSE UNDER VARIOUS LASER CONDITIONS

As discussed in Section I A on the sources of prepulse, prepulse is expected to have a dependence on the condition of the amplifier windows as well as on amplifier loading. Experimental results on the effect of these conditions as well as the absolute prepulse levels under standard operation are presented in this section. Throughout, $t = 0$ refers to the time at which the laser pulse reaches 1/2 of its peak intensity.

A. Standard operation

Typical measured prepulse under standard laser operation is shown Figure 6. As can be seen in the figure, prepulse rises sharply until $t = -130$ ns, and then levels off at $\sim 10^7$ W/cm^2, until approximately $t = -10$ ns, after which time the pulse-shape is determined by the laser front end. Prepulse first rises above the noise at approximately $t = -150$ ns, just after the expected beginning of 20 cm ASE (Section I A 1). The time integral of the intensity up to $t = -10$ ns gives the prepulse energy density on target of approximately 2-3 J/cm^2 in this case. The Figure also shows the calculated ASE, which is nearly an order of magnitude below the measured prepulse. As discussed in Section I A 1, this is expected since the calculation assumes saturated gains for the amplifiers and does not include BBS.

Also plotted is the simulated ASE intensity. The simulation is in good agreement with the measured rise of the prepulse between $t = -150$ and -120 ns. After $t = -120$ ns, the measured prepulse is somewhat higher than the simulated ASE, as is expected due to the start of BBS at approximately $t = -120$ ns. The simulated ASE includes the initial spike in gain before the amplifiers are loaded by the laser beams and thus is higher than the ASE estimate based on saturated gains until approximately $t = -32$ ns.

B. Effect of ASE suppression

As discussed in Section I A 1, ASE emitted during amplifier ramp-up is expected to be a significant contributor to prepulse. In order to observe this effect, the level of ASE during ramp-up of the 20cm amplifier was changed by delaying its firing by 20 ns. In the delayed case, the amplifier is loaded by the input beams during most of the ramp-up, suppressing ASE during that time. Figure 7 shows the effect of the 20 ns delay on ASE emission from the amplifier. As can be seen in the figure, the delayed firing strongly suppresses the initial emission while increasing the ASE toward the end of the amplifier pulse. The latter, however, does not contribute to the prepulse because emission during that late time arrives on target after the laser beams.

The effect of suppressing the 20cm ASE during the ramp-up is shown in Figure 8. Prepulse level decreases nearly an order of magnitude for $t < -50$ ns as a result of the suppression. It can be concluded that 20cm ASE produced during the ramp-up is a very significant part

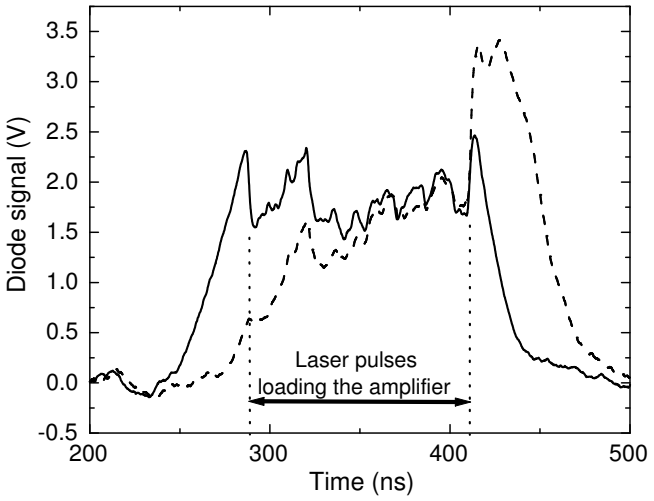

FIG. 7: Suppression of 20cm amplifier ASE by delaying the amplifier firing. The traces show off-angle 248 nm emission (ASE as well as BBS) from the 20cm amplifier as recored by a photodiode located at an angle w.r.t the collection optics for the individual beams. The time between the two vertical dotted lines is when the amplifier is loaded by the multiplexed laser pulses passing through it. The solid trace corresponds to standard amplifier timing; the dashed trace – to the 20cm amplifier firing delayed by 20 ns. In the latter case the amplifier is loaded during its ramp-up, decreasing the ASE that can arrive on target early as prepulse. Note: here $t = 0$ does not correspond to the half-rise of the main pulse on target.

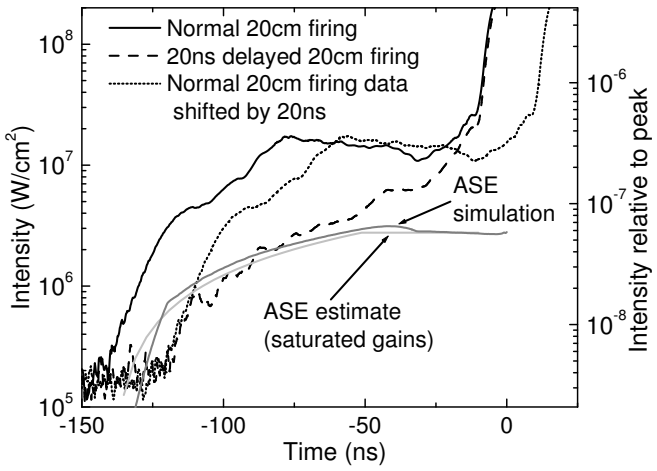

FIG. 8: The effect of suppression of 20cm amplifier ASE. The solid trace is an average of 3 shots with standard amplifier timing. The dashed trace is an average of 2 shots with the 20cm amplifier firing delayed by 20 ns. In the latter case the amplifier is loaded during its ramp-up, decreasing the ASE. The standard amplifier timing data is also plotted with a 20 ns shift (dotted line) to show that prepulse decrease is not just due to the 20 ns delay in the amplifier turn-on. Also shown is the ASE simulation for delayed firing (gray trace), as well as a theoretical estimate of the prepulse from ASE assuming saturated gain in the amplifiers (light gray trace). All shots are with 19 beams and new windows on both the 20cm and the 60cm amplifiers. The 8 ns delay of the rise of the measured prepulse with respect to the ASE simulation is due to the last two beams in the 20cm amplifier train not being part of the 19 beams used in these shots.

of the prepulse. The time the ASE comes up above noise in this measurement is just after the earliest ASE on target expected from the 20cm amplifier. As discussed in Section I A 1, it is the time difference between the 20cm amplifier ramp-up and the last beam going through the amplifier. The 20cm ASE is thus expected to begin at -155 ns with normal 20cm timing and at -135 ns with the 20ns delayed firing. The measurement shows the prepulse rising above the noise level just after these times.

Also plotted in the figure are the ASE estimate using saturated gains and the ASE simulation for the 20 ns delayed firing of the 20cm amplifier. It is apparent that in this case the measured prepulse and the ASE simulation are close to the prepulse level expected from just the saturated amplifier gains, indicating that the delayed firing had suppressed the unloaded amplifier gain spike normally present at the amplifier startup, as expected. The measured prepulse is still above that computed from the ASE simulation due to BBS.

C. Effect of amplifier window condition

The effect of replacing the windows on the final (60cm) amplifier is shown in Figure 9. The difference is within shot-to-shot variation. This indicates that BBS at the final amplifier is not a significant component of the total prepulse, at least under the condition of old 20cm amplifier windows.

The effect of replacing the 20cm amplifier windows is shown in Figure 10. These shots were taken with the 20 ns delayed firing of the 20cm amplifier. Under this condition, the measured prepulse level is an order of magnitude lower with the newly polished windows than with the heavily used ones. This demonstrates that BBS at the 20cm amplifier is an important contributor to prepulse. With standard timing of the 20cm amplifier, the effect of the windows replacement would not be as dramatic, since the ASE during ramp-up would not be suppressed.

D. Earliest prepulse measurement

Prepulse levels down to 10^{-10} from the peak laser intensity can be measured using the diagnostic setup. Figure 11 shows that the earliest measurable prepulse occurs starting at approximately $t = -280$ ns. This is as expected from the time difference between the 60cm amplifier turn-on and the last beam entering the amplifier, as discussed in Section I A 1. The second sharp rise in the prepulse at approximately -135 ns corresponds to the

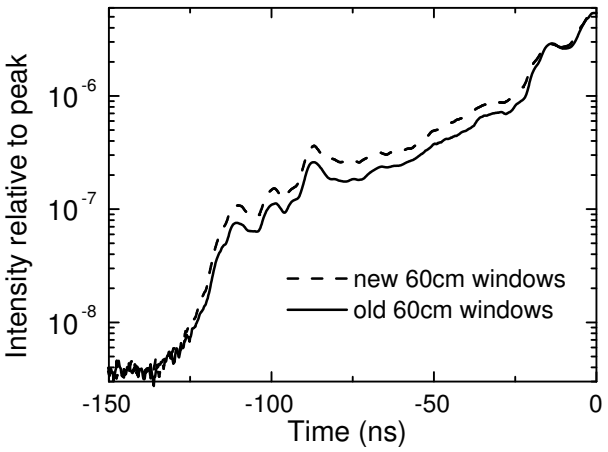

FIG. 9: The effect of replacing etched 60cm amplifier windows with newly polished ones is not significant. The solid trace is the average of 6 shots with the old 60cm windows; the dashed trace is an 8 shot average with new 60cm windows. The difference is within shot-to-shot variation. All shots were with 19 beams, old windows on the 20cm amplifier, and 20 ns delayed firing of the 20cm amplifier.

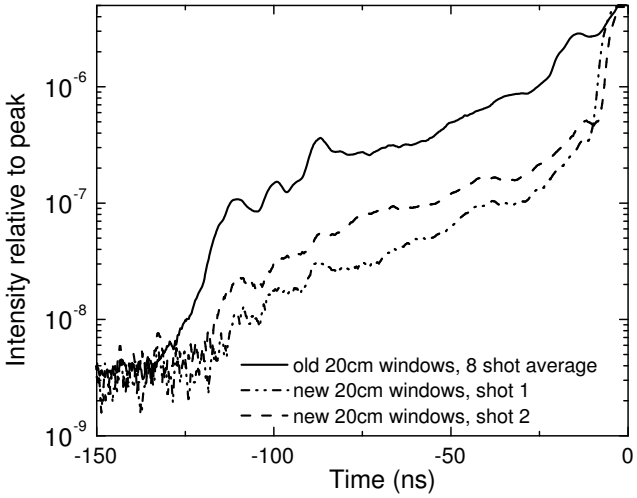

FIG. 10: The effect of replacing etched 20cm amplifier windows with newly polished ones. The solid trace is the average of 8 shots with the old 20cm windows; the dashed traces are two individual shots with new 20cm windows. All shots were with 19 beams, new windows on the 60cm amplifier, and 20 ns delayed firing of the 20cm amplifier.

expected start of the 20 cm ASE with the 20 ns delayed firing. Once again, the calculated prepulse level due to ASE from the 60cm amplifier is an order of magnitude below the measured total prepulse as the calculation assumes saturated gain and does not include BBS. Also shown is the simulated 60cm ASE which includes the unloaded gain spike. It is closer to the measurement, but,

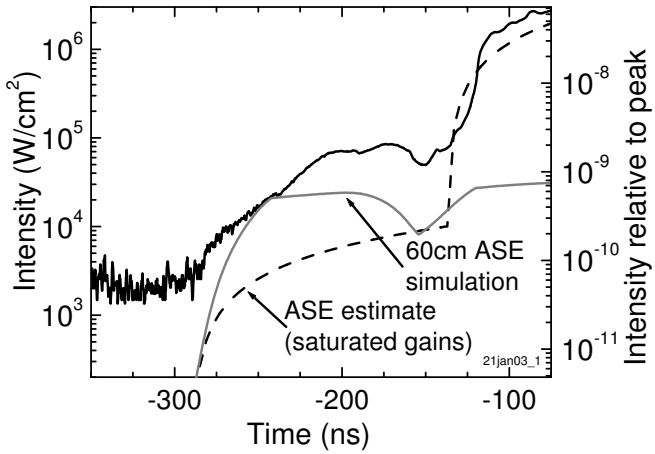

FIG. 11: Earliest prepulse measurement. 19 beams, new windows on the 60cm amplifier, old windows on the 20cm amplifier, and 20 ns delayed firing of the 20cm amplifier. The measured prepulse (solid black trace) shows distinct contributions from the 60cm and 20cm amplifiers, starting at approximately -280 ns and -130 ns, respectively. The dashed trace shows the calculated ASE assuming saturated gain of the amplifiers. The gray trace shows a simulation of the ASE from the 60cm amplifier.

as expected, measured prepulse rises after $t = -240$ ns due to the start of BBS in the 60cm amplifier.

E. Comparison of direct prepulse measurements to pulseshape diagnostics on individual beams

As mentioned in the introduction, low level prepulse is measured at full power for several individual beams by light pickoff. These diagnostics measure intensity relative to the peak for that individual beam. They can be used to monitor prepulse on regular target shots, when direct prepulse measurement on target is not available. In order to compare these individual beam measurements to the prepulse intensity measured directly on target, shots were taken with only one of such measured beams on target at a time. An example is shown in Figure 12. As seen on the figure, there is good agreement between the prepulse measured directly on target and that measured by light pickoff on the same beam. Differences in the two waveforms are probably due to the higher time resolution of the pickoff measurement: ~ 100 ps vs. ~ 3 ns for the on target measurement.

IV. DISCUSSION

As shown above, prepulse has been measured to be $\sim 2 \times 10^{-7}$ from peak for approximately 120 ns prior to the main laser pulse under standard operating conditions. Prepulse energy density on target is approximately $2 - 3$ J/cm^2. This prepulse level is probably

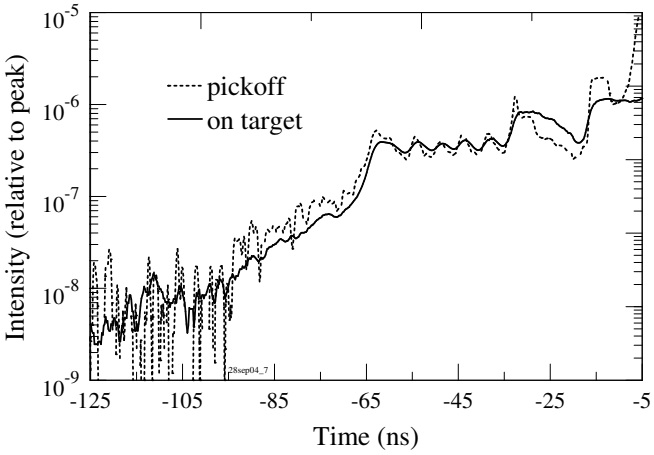

FIG. 12: Prepulse for a single beam as measured on target (solid line) and by light pickoff from the beam (dotted line).

insufficient to result in significant preheating of a plastic target, where the absorption depth for 248 nm is ~ 2 μm. It could, however, be significant for targets coated with thin (~ 400 Å), low heat capacity metallic coating, such as those used for imprint suppression[3]. Since most of the prepulse light is absorbed in the metallic coating, this could result in significant preexpansion of the coating. It remains to be seen whether preexpansion plays a significant role in target dynamics after the arrival of the laser pulse. A possible benefit to preexpansion could be increased separation between the laser absorption surface and the ablation surface, decreasing the imprinting of laser non-uniformity onto the target.

The minimum prepulse energy density required to affect a target with a 400 Å gold layer would be on the order of the energy density required to vaporize the metallic layer. An estimate of this can be made as follows. Areal mass density of the gold layer is 19.3 g/cm^3 $\times$ 400 Å $\times$ 10^{-8} cm/Å $= 7.7 \times 10^{-5}$ g/cm^2. The boiling point, heat of fusion, and heat of vaporization of gold are 3130 K, 64.6 J/g, and 1650 J/g, respectively [11]. Taking the heat capacity to be that at 25°C, 0.13 J/g K, the estimated energy density needed to vaporize the coating is

$$7.7\times10^{-5}\ \mathrm{g/cm^2}\ (0.13\ \mathrm{J/g{\cdot}K} \times 3130\ \mathrm{K} + 64.6\ \mathrm{J/g} + 1650\ \mathrm{J/g}) = 0.16\ \mathrm{J/cm^2} \quad (9)$$

The thin metallic layer is thus expected to be affected by the prepulse since the measured prepulse is an order of magnitude higher than this estimate.

Prepulse measurements were also conducted with ASE suppression by a change in amplifier timing, as well as under the conditions of heavily used amplifier windows. As expected from the discussion on the sources of prepulse in Section I A, prepulse has been found to depend strongly on the ASE suppression and window condition of the 20cm amplifier. Loading the amplifier 20 ns earlier results in a significant decrease in the prepulse level. Under this condition of reduced ASE, the heavily used 20cm amplifier windows result in an almost an order of magnitude increase in prepulse level. The latter underscores the need for timely window replacement if minimizing prepulse is important. The former indicates that use of auxiliary beams from the laser front end to load the amplifier as it is ramping up would significantly decrease the prepulse level on target.

Though the use of auxiliary beams to suppress ASE requires installation of additional optics, it is advantageous over the ASE suppression by delaying amplifier firing for the following reasons. With the delayed amplifier firing, the first few beams would see lower gain and thus would have lower energy than with the normal firing of the amplifier. Additionally, the energy in these beams would become sensitive to the jitter in the firing of the amplifier and would vary shot-to-shot. Auxiliary "throw-away" ASE suppression beams are thus a more desirable approach to ASE suppression. Use of such beams is currently being implemented on Nike.

V. CONCLUSIONS

We have presented the first direct full power measurements of prepulse on target on the Nike laser. The diagnostic developed for this purpose is able to measure prepulse levels as low as 10^{-10} from peak laser intensity. Under standard operating conditions, prepulse is found to be $\sim 2 \times 10^{-7}$ from peak for approximately 120 ns prior to the main laser pulse. Prepulse energy density on target is approximately $2 - 3$ J/cm^2.

As expected from theoretical considerations, the 20cm amplifier was found to be the dominant source of prepulse: the condition of the amplifier windows as well as suppression of ASE produced on ramp-up have significant effects on the prepulse intensity on target.

Acknowledgments

The authors would like to thank the Nike laser and target crews for their help in these experiments, especially laser operators Steve Terrell and Zeb Smyth for operating the laser under various conditions. The authors would also like to thank the referee for their numerous helpful suggestions on improving the manuscript. This work was supported by the U.S. Department of Energy, NNSA-Defense Programs.

[1] S. E. Bodner, D. G. Colombant, J. H. Gardner, R. H. Lehmberg, S. P. Obenschain, L. Phillips, A. J. Schmitt, J. D. Sethian, R. L. McCrory, QW. Seka, C. P. Verdon,

J. P. Knauer, B. B. Afeyan, and H. T. Powell. Direct-drive laser fusion: Status and prospects. *Phys. Plasmas*, 5(5):1901–1918, May 1998.

[2] S. P. Obenschain, S. E. Bodner, D. Colombant, K. Gerber, R. H. Lehmberg, E. A. McLean, A. N. Mostovych, M. S. Pronko, C. J. Pawley, A. J. Schmitt, J. D. Sethian, V. Serlin, J. A. Stamper, C. A. Sullivan, J. P. Dahlburg, J. H. Gardner, Y. Chan, A. V. Deniz, J. Hardgrove, T. Lehecka, and M. Klapisch. The Nike KrF laser facility: Performance and initial target experiments. *Phys. Plasmas*, 3(5):2098–2107, May 1996.

[3] S. P. Obenschain, D. G. Colombant, M. Karasik, C. J. Pawley, V. Serlin, A. J. Schmitt, J. L. Weaver, J. H. Gardner, L. Phillips, Y. Aglitskiy, Y. Chan, J. P. Dahlburg, and M. Klapisch. Effects of thin high-Z layers on the hydrodynamics of laser-accelerated plastic targets. *Phys. Plasmas*, 9(5):2234–2243, May 2002.

[4] M. Nantel, J. Itatani, A.-C. Tien, J. Faure, D. Kaplan, M. Bouvier, T. Buma, P. Van Rompay, J. Nees, P. P. Pronko, D. Umstadter, and G. A. Mourou. Temporal contrast in Ti:Sapphire lasers: Characterization and control. *IEEE J. Sel. Top. Quant. Elect.,*, 4(2):449–458, 1998.

[5] A.-C. Tien, M. Nantel, G. Mourou, D. Kaplan, and M. Bouvier. High-dynamic-range laser-pulse-contrast measurement with a plasma-shuttered streak camera. *Opt. Lett.*, 20(22):1559–1561, Oct. 1997.

[6] M. Karasik, E. A. McLean, and J. A. Stamper. Studies of target heating in the early stages of a Nike KrF laser pulse. In *Bull. Amer. Phys. Soc.*, number 7, page GP1.78, October 2000.

[7] M. W. McGeoch, P. A. Corcoran, R. G. Altes, I. D. Smith, S. E. Bodner, R. H. Lehmberg, S. P. Obenschain, and J. D. Sethian. Conceptual design of a 2-MJ KrF laser fusion facility. *Fusion Technol.*, 32:610–643, Dec. 1997.

[8] J. L. Giuliani, P. Kepple, R. H. Lehmberg, M. C. Myers, J. D. Sethian, M. F. Wolford, F. Hegeler, and G. Petrov. Orestes: a kinetics model for electron beam pumped KrF lasers. In B. A. Hammel, D. D. Meyerhofer, J. Meyer ter Vehn, and H. Azechi, editors, *Third Inertial Fusion Sciences and Applications*, pages 580–3. American Nuclear Society, 2003. Paper WPo4.31.

[9] J.A. Sullivan, G.R. Allen, R.R. Berggren, S.J. Czuchlewski, D.B. Harris, M.E. Jones, B.J. Krohn, N.A. Kurnit, W.T. Leland, C. Mansfield, J. Mcleod, A.W. Mccown, J.H. Pendergrass, E.A. Rose, L.A. Rosocha, and V.A. Thomas. KrF amplifier design issues and application to inertial confinement fusion system design. *Laser Part. Beams*, 11(2):359–383, 1993.

[10] Y. Owadano, I. Okuda, Y. Matsumoto, I. Matsushima, K. Koyama, T. Tomie, and M. Yano. Performance of the ASHURA KrF laser and its upgrading plan. *Laser Part. Beams*, 11(2):347–351, 1993.

[11] D. R. Lide, editor. *CRC Handbook of Chemistry and Physics*. CRC Press, internet version, 84th edition, 2004.